ELSEVIER

Calculations of diffusion and diffusion-limited processes in Ni₃Al using accelerated molecular dynamics

Colin Harris [a], Raymond Tedstrom [a], Murray S. Daw [a,*], Michael J. Mills [b]

[a] *Department of Physics and Astronomy, Clemson University, Clemson, SC 29634, United States*
[b] *Department of Materials Science and Engineering, The Ohio State University, Columbus, OH 54321, United States*

Abstract

We present a systematic microscopic approach to diffusion and diffusion-limited processes in Ni₃Al. These processes have been identified as controlling the deformation of the material under specific circumstances. The embedded atom method calculations are done using kinetic Monte Carlo combined with the Dimer method of finding saddlepoints. We compute the tracer diffusivities as functions of composition and temperature. The comparison with available experiments is good. We find that at temperatures below about 1000 K, the diffusivity is a sharp function of composition, showing a pronounced dip on the Ni-rich side at 76 at.% Ni. This agrees well with experiment, except that the experiments show this structure setting in a temperatures below about 1300 K. We show that the structure arises from the composition dependence of both the vacancy formation energy and pre-exponential of the diffusivity. We also compute the mobility of an anti-phase boundary perpendicular to its plane, and conclude that vacancy-assistance is very plausible. We conclude that the kMC + Dimer method works well for these problems above 700 K but less effectively below, owing to the presence of short-range, low-energy hops that tend to localize the vacancy and lower the efficiency of the calculation.
© 2005 Elsevier B.V. All rights reserved.

1. Introduction

Detailed microstructural analysis of deformation mechanisms in intermetallic alloys have revealed several interesting diffusion-limited processes. Generally speaking, classic dislocation climb has long been identified as a very important process controlling deformation of intermetallics [1]. However, several unusual processes have been identified by more recent work.

For example, the translation of Anti-Phase Boundaries (APBs) was observed by Rong et al. [2] in Ni₃Al. They found that, during creep, edge dislocations commonly dissociated perpendicular to the slip plane. They concluded that the formation of that configuration limited the extent of primary creep deformation. Moreover, it is presumed that the APB can be translated perpendicular to itself,

and that it moves via microscopic mechanisms similar to that which control long-range diffusion (that is, vacancy-assisted).

Srinivasan et al. [3] identified in NiAl a pairing of dislocations which move together by the exchange of vacancies, one acting as a source and the other a sink. The pair results from the partial decomposition of a parent dislocation. The coupling via short-range diffusion keeps the products together. Each partner is climbing, and the overall effect is to accomplish glide of the combination.

Srinivasan et al. [4] identified a similar coupling of climb-dissociated superpartials in Ni₃Al (see Fig. 1). The superpartials are moving on non-parallel glide planes. Overall glide of the pair is accomplished by the exchange of vacancies between the partners. This case is made even more interesting because the partners are tethered by an APB: the motion of the pair also requires the translation of the APB perpendicular to its plane.

The climb-dissociated pair of Fig. 1 embodies two aspects of interest in the present work. First, the combined

---

* Corresponding author.
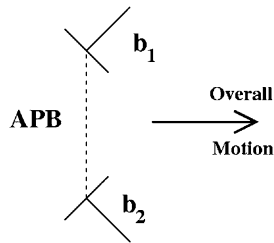 *E-mail address:* daw@clemson.edu (M.S. Daw).

Fig. 1. Motion of climb-dissociated pair. See [4].

climb–glide process is controlled by a dipole (that is, source and sink) diffusion problem. The rate of motion of the pair may be limited by diffusion. Second, the translation of APB must be accomplished, and the detailed mechanism of this has not been considered in the literature. It may be that the APB motion is the slower process in this case.

Underlying the coupled sink–source and APB translation problems is the problem of diffusion in an ordered lattice. Diffusion in ordered intermetallics has been an active area of investigation in its own right [5]. Many authors have investigated the role of vacancies, and posed various possible microscopic mechanisms that may dominate. The obvious interplay between diffusion and lattice order makes it clear that the dominance of one mechanism over another depends on the amount of order. Experiments are available for Ni tracer diffusivity and chemical diffusivity at higher temperatures, but not for Al tracer diffusivity or at lower temperatures.

Interestingly, the published theoretical work includes an omission of very much traditional Molecular Dynamics, pointing to the fact that the general theoretical problem here is one of disparate time scales (much more so that length scales): diffusion is very slow compared to lattice vibrations. Recent developments in Accelerated Molecular Dynamics (AMD) [6] have overcome many of the difficulties associated with traditional MD, in that simulations over much longer effective time scales are now possible in some cases.

We aim here to take the first step toward a direct simulation of the diffusion-limited processes in intermetallics using AMD. There are several flavors of AMD. The one most appropriate here is kinetic Monte Carlo combined with saddlepoint search using the Dimer method. This on-the-fly kMC works well for the case of a single vacancy in a somewhat disordered intermetallic because the diffusion consists largely of discrete jumps from one energy valley to another, with a well-defined number (always 12 in the present application) of possible saddlepoints exiting a valley. We report here the first approach to the problem of diffusion-limited processes using accelerated MD techniques.

The energetics for the kMC is obtained in this paper by the Embedded Atom Method (EAM) [7], which is a semi-empirical many-atom description of metallic bonding. The EAM has been demonstrated to yield reliable results for close-packed metals and alloys, and has been applied

previously to the Ni$_3$Al alloy under consideration in this work, with good results [8,9].

This paper begins with a brief description of the technique, which has become well-known. Then we show two applications. The first problem addressed is that of bulk tracer diffusivities as functions of temperature and composition. The second problem is the translation of an anti-phase boundary perpendicular to itself. Both problems illustrate the power and limitations of the kMC + Dimer approach, which we discuss at the end of the paper.

2. Method: on-the-fly kinetic Monte Carlo

Kinetic Monte Carlo has been a useful tool for decades (see, for example, [10]). Where there are well-defined valleys in the energy surface separated by simple saddlepoints, the approach lists all the exits from a valley with an associated probability $p_i = \exp(-\Delta E_i/k_B T)$ where the ΔE_i is the energy barrier to be crossed for that exit. From that list is then selected, randomly according to the weights p_i, a single exit. That exit is taken, leading to a new valley, and the time is incremented by $dt = \tau \exp(+\Delta E_i/k_B T)$. In the present work, the overall time scale τ of Monte Carlo steps will be determined by fitting to one experimental data point later.

Kinetic Monte Carlo is usually implemented with a pre-defined event table. However, if the necessary saddle-point energies cannot be categorized in a simple way, then it may become necessary to calculate saddlepoint energies on-the-fly (see, for example, [11]). In the present calculation, because of the effects of temperature and stoichiometry, we are concerned with the influence of anti-site defects on vacancy migration. We tested the dependence of vacancy migration saddlepoint energies in $L1_2$ on the positions of possible anti-site defects among the neighbors of the vacancy. We found that even fifth neighbors of the vacancy can have non-negligible effects on the saddlepoint energies. This is understandable if one considers neighbors of the atom which is exchanging with the vacancy: a second neighbor of that atom is a fifth neighbor to the vacancy. This means that in constructing a pre-defined event table, one must consider various configurations of anti-site defects out to fifth neighbors of the vacancy. The number of possible configurations in that case is quite large, making a pre-defined event table impractical.

Furthermore, our eventual goal is to carry out calculations of diffusion-limited processes in more complex possibilities; consider the complexity of microscopic configurations present during the climb of an edge dislocation or during the motion of the pair pictured in Fig. 1. Even if the pre-defined event table would work for the problem of bulk diffusion, we would eventually have to discard it when going to more complex problems. This paper then aims at the development of AMD, and uses bulk diffusion as a good starting point.

We need then to find the saddlepoints for each configuration. This is an ideal situation for the Dimer method,

which can be used as an efficient means of locating exits from a valley. We have implemented the Dimer method in much the same way as previous authors, although we have found it somewhat more efficient to isolate a small sub-space for the Dimer rotation step.

We have also tested out the use of a "history" table. This is a catalog of all the local configurations (out to fifth neighbors) sampled by the vacancy; with each entry is stored the saddlepoints that were found. In this sense, we are actually performing a hybrid between the pre-defined event table and the on-the-fly, in that we accumulate an event table based on how the calculation unfolds. We find that there is some savings using the history table, especially when there is some oscillation between a small number of related configurations. In that sense, we have the best of both worlds, because we only need to compute saddlepoints for configurations that are actually sampled by the vacancy. However, we note that in the calculations of APB mobility, the rich variety of environments is so large that the history table presents only a modest improvement in efficiency.

We have used the Voter–Chen EAM functions for Ni_3Al [9]. As we will note below, these functions present largely reliable results, with the exception that the vacancy formation energies appear to be about 0.3 eV too low as compared to experiment. Otherwise, the results obtained in the present work compare very well with experiment.

It should be noted that we do not account for thermal expansion: all calculations are done at the same lattice constant. This is because we wanted to test the efficiency of the "history" table, but the payoff was marginal. We do not expect that neglecting the change in lattice constant will greatly change the conclusions of the work.

3. Bulk tracer diffusivities

To calculate bulk tracer diffusivities, we created a cube with 863 atoms and 1 vacancy. We populated the lattice with population drawn from Ni_xAl_{1-x}. We ran configurations with values of $x = 0.7, 0.725, 0.75, 0.775, 0.8$ at temperatures of $T = 300, 600, 900, 1200, 1500, 1800$ K. At each composition and temperature, we ran 5000 iterations, and used sub-averaging to determine statistical errors.

Off-stoichiometric simulations below $T = 900$ K resulted in certain peculiarities. During Al-rich low temperature runs, the vacancy was often observed to become stuck between a set of 2 or 3 valleys for entire simulations. During Ni-rich low temperature simulations, results were found to change significantly based upon the initial conditions. These particular simulations must be analyzed more closely before any conclusions can be made; therefore we do not include them in our present results.

The reader should keep in mind that the vacancy concentration is fixed at 1 in 864. Because we assume that the tracer diffusivities are proportional to the vacancy concentration, we will have to correct our values by compensating for the equilibrium vacancy concentration. However, the results we
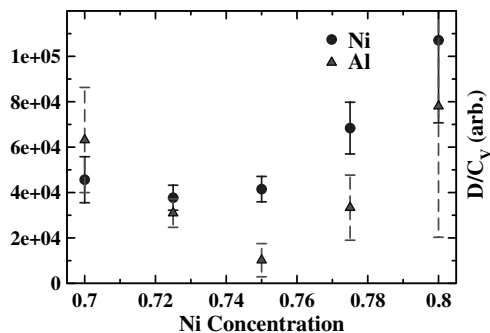
Fig. 2. Calculated tracer diffusion coefficients as functions of stoichiometry at $T = 1200$ K. The tracer diffusion is calculated at a fixed vacancy concentration of 1/864. The statistical error bars have been computed by sub-averaging.

obtain at first are uncorrected, and so we will presented them as D/C_V.

We show the result of (uncorrected) tracer diffusivities at $T = 1200$ K and various x (see Fig. 2). These results are typical of the other temperatures in that Ni is usually more mobile, and the Al diffusivities carry higher statistical error, because they are more sensitive to the presence of defects.

It is interesting to look at the histogram of saddlepoints the vacancy samples during the simulations (see Figs. 3 and 4) At low temperatures and ideal stoichiometry, the vacancy moves predominantly on the Ni sublattice and has 8 Ni neighbors and 4 Al neighbors, so that the
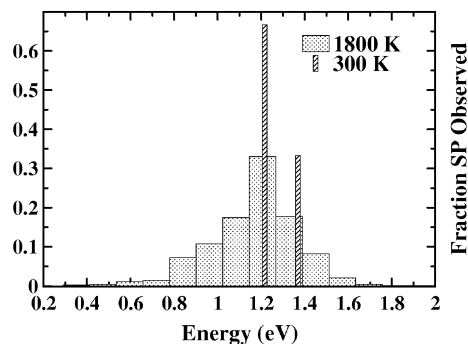
Fig. 3. Saddlepoint energies observed by a vacancy for $x = 0.75$ at $T = 300$ K and $T = 1800$ K.
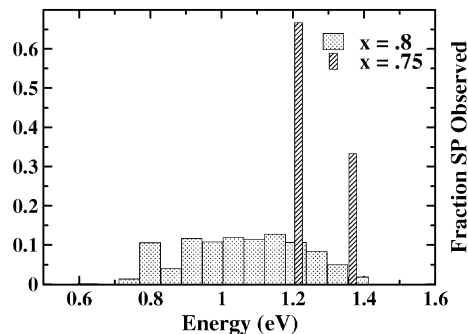
Fig. 4. Saddlepoint energies observed by a vacancy for $x = 0.75$ and $x = 0.8$ at $T = 300$ K.

histogram shows two dominant saddlepoint energies at about 1.2 eV and 1.4 eV for the interchange of the V with a neighbor Ni and Al, respectively. Raising the temperature significantly (Fig. 3) broadens the distribution of the saddlepoints that the vacancy chooses from because of the higher population of anti-site defects. The distribution is centered at about 1.2 eV but samples almost 0.6 eV lower and higher. Changing the stoichiometry (but keeping the temperature low) (Fig. 4) also significantly broadens the distribution, and furthermore lowers the center of the distribution to about 1.0 eV.

With this significant broadening in the distribution of saddlepoints sampled by the vacancy, one is tempted to ask whether the diffusion will in fact have a simple Arrhenius behavior. The answer is apparently that the diffusivity is still simply Arrhenius, which can be seen by the Arrhenius plot (and fit) of our kMC results (Fig. 5). Because we are holding the vacancy concentration fixed, the temperature dependence is appropriately characterized by a migration energy.

Tracer experiments by Shi et al. consistently show deviation from Arrhenius behavior at 1200 K (their lowest temperature). Although a few of our results show deviation from the Arrhenius behavior, high statistical errors do not allow us to confirm or deny such a result.

Fitting all of our data shows how the migration energy depends on composition (Fig. 6). It is not surprising that E_{mig}^{Al} is peaked at ideal stoichiometry. A microscopic analy-

sis of the motion of the Al atoms shows that the Al cannot move effectively on the Al sublattice. For Al-rich compositions, the promotion of Al to the Ni sublattice allows Al to move more freely. For Ni-rich compositions, even the small presence of Ni on the Al sublattice allows greater freedom for the Al to move. Examining the motions of the atoms during the simulations confirms that the principle diffusion mechanism is intra-sublattice (ISL). However, we have not sufficiently investigated (as was noted above) the regime of non-ideal stoichiometry and low temperature, which might reveal a different mechanism at play.

We conclude from these results that even though a broad distribution of saddlepoint energies is sampled by the vacancy, the net effect is for simple Arrhenius behavior. This may be due in part to the fact that many of the events available at low energy do not contribute to long-range diffusion of the elements, but instead involve only local shuffling of constituents.

Now, these calculations were done at fixed vacancy concentration (1 in 864). However, assuming that the diffusivity should be strictly proportional to vacancy concentration, this is easy to correct for. (Note that by construction divacancy processes are excluded from our calculation. This is not a fundamental limitation of the present method.) We begin by calculating the point defect energies and applying statistical mechanics (Ref. [8]). From this procedure we can calculate the predicted vacancy concentration as a function of temperature and composition (see Fig. 7). We find that V_{Al} is uncommon. At $T = 1500$ K, the vacancy concentration shows some dependence on composition. Convolving this with our calculated diffusivities at fixed vacancy concentration, we can form our predicted tracer diffusivities and compare to experiment.

Fig. 8 shows the comparison. Note that only the Ni tracer diffusivity is experimentally accessible (a suitable isotope for Al is not readily available). Experiments have been conducted using In as a substitute for Al (Ref. [12]). Our results for the tracer diffusivity of Al do not agree well with the results obtained for In.

Note that there is one point which is used as normalization for the theory. This free parameter comes from the time-scale of the kMC jumps which we have not determined. We adjust this kMC time-scale to match the
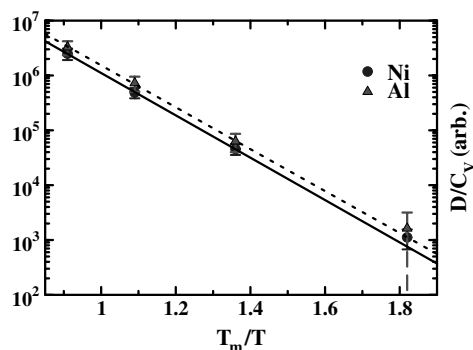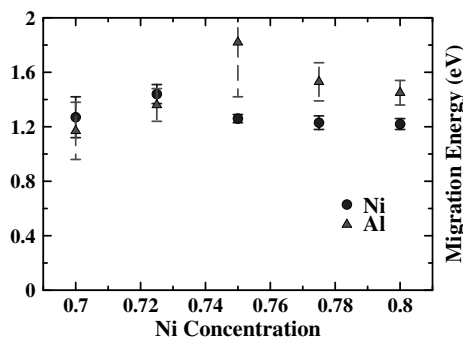

Fig. 5. Arrhenius plot at $x = 0.7$.
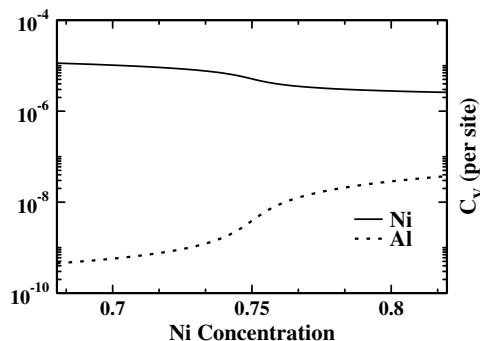

Fig. 6. Migration energy vs. composition.

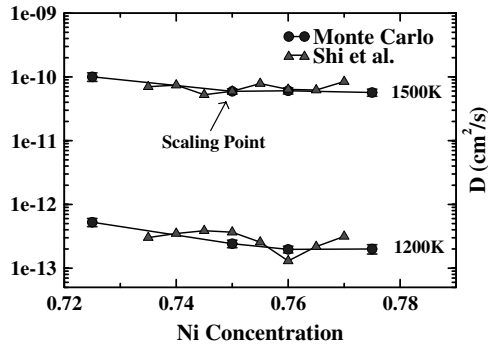Fig. 7. Calculated equilibrium vacancy concentration at $T = 1500$ K.

Fig. 8. Comparison of calculated tracer diffusivities (at equilibrium vacancy concentrations) to experimental data, at $T = 1500$ K and $T = 1200$ K. The theoretical diffusivities have one parameter, which is fixed by forcing agreement to this experiment at $x = 0.75$ and $T = 1500$ K. See Ref. [12].

Fig. 10. Predicted Ni tracer diffusivity as a function of stoichiometry for $T = 1500$ K, $T = 1200$ K and $T = 900$ K.

Fig. 11. Predicted Al tracer diffusivity as a function of stoichiometry for $T = 1500$ K, $T = 1200$ K and $T = 900$ K.

measured Ni tracer diffusivity at $T = 1500$ K and $x = 0.75$, giving a value of $\tau = 0.8$ ps. The rest of the calculated points are then predictions.

Certainly there is general agreement between the theoretical and experimental results in the dependence of tracer diffusivities on stoichiometry.

To investigate the effects of temperature we now go through the same process at a lower temperature, $T = 900$ K which is a temperature of considerable interest to those studying deformation of this alloy. We begin by calculating the vacancy concentration at this temperature, which is shown in Fig. 9. By contrast to the vacancy concentration at higher temperatures, we see now a very abrupt change with stoichiometry that occurs near the ideal composition. Convolving the vacancy concentration at this temperature with the calculated kMC + Dimer results also at this temperature gives us a prediction for the tracer diffusivities as a function of stoichiometry in Figs. 10 and 11. Here we see that the tracer diffusivities are more sensitive functions of the stoichiometry, so that the diffusion-limited processes may occur several times faster in Al-rich samples than in Ni-rich samples. This effect, while not huge, certainly should be measurable.
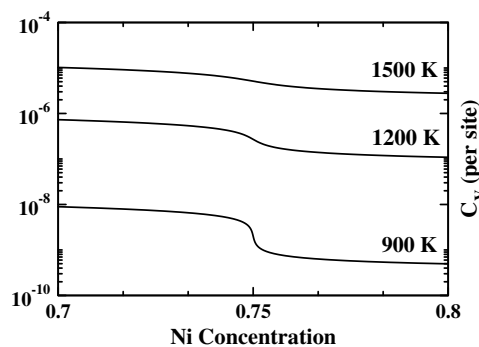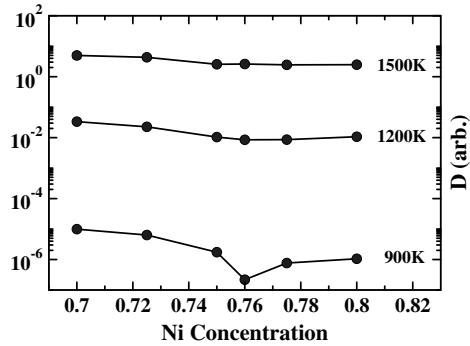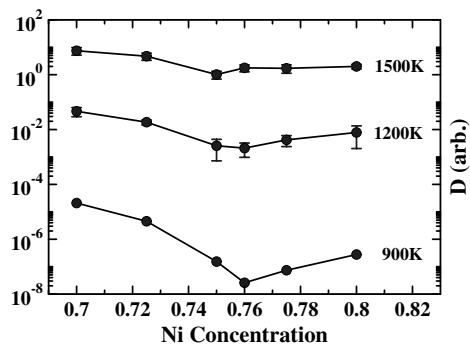
In tracer experiments conducted by Shi et al. a defined minimum in Ni diffusivity was found at $x = 0.76$ for temperatures below 1400 K. This minimum becomes more distinct as the temperature decreases. It is now clear that the creation of this offset minimum is due to two competing factors. The first is the increase of diffusivity *at constant vacancy concentration*, which is seen in Fig. 2 for compositions above ideal stoichiometry. This increase is due primarily to the increase in pre-exponential, because the migration energy is relatively independent of composition, as shown in Fig. 6. The second factor is the decrease in vacancy concentration, as shown in Fig. 7. These two factors lead to a dip in the diffusivity at $x = 0.76$. As the temperature is decreased the change in vacancy concentration about ideal stoichiometry becomes more abrupt, causing this observed minimum to become more distinct (see Fig. 10). This minimum is also observed in the diffusivity of Al as a function of composition at $x = 0.76$ (see Fig. 11). Our calculations show this minimum to become significant at 900 K where as results from Shi et al. show this to happen around 1200 K. The reason for the difference in temperature between theory and experiment appears to arise from the calculated vacancy formation energy, which for the Voter–Chen EAM functions is slightly low compared to experiment.

Accounting for vacancy concentrations, we can also make a comparison of activation energies with experiment.

Fig. 9. Calculated equilibrium vacancy concentration at $T = 1800$ K, $T = 1500$ K, $T = 1200$ K and $T = 900$ K.
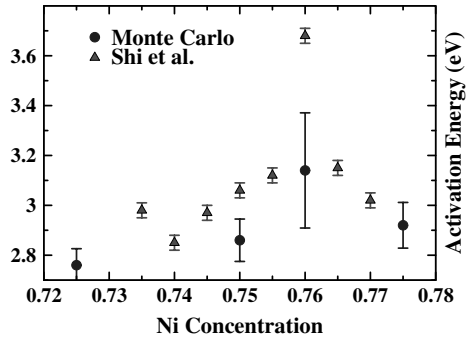
Fig. 12. Comparing activation energies to experiment.

Additional simulations were conducted in an attempt to observe a maximum in the activation energy at $x = 0.76$ observed by Shi et al. (Fig. 12). We find the same maximum, however our values are consistently lower than experiment. Previous work in our group using the same EAM functions found a formation energy for V_{Ni} to be approximately 0.3 eV *lower* than the most recently reported experimental value [13]. This accounts for the consistent discrepancy between theory and experiment in the activation energies. An incorrect formation energy is also the reason we find a distinct minimum in diffusivity vs. composition to occur at a *lower* temperature than experiment.

To conclude our discussion of bulk tracer diffusivities in Ni₃Al, we find that:

- Diffusion occurs primarily in the Ni sublattice.
- The diffusivity follows a largely Arrhenius behavior.
- The dependence on stoichiometry agrees with experimental measurements at $T = 1500$ K and $T = 1200$ K.
- The prediction for diffusivities at $T = 900$ K shows a pronounced dependence on stoichiometry, with a minimum at $x = 0.76$, in agreement with experiment.
- The dip in diffusivity for Ni-rich compositions arises from two effects. The first is that the diffusivity at constant vacancy concentration increases with x above 0.75. The second is that the vacancy concentration drops rapidly with concentration in the same range. The combination results in a minimum in the overall diffusivity at $x = 0.76$.

4. Translation of an anti-phase boundary

Returning to the climb-dissociated pair which motivated this work (Fig. 1), we would like to investigate the microscopic mechanism which allows the translation of an APB perpendicular to itself, and also estimate the speed of this translation, and dependence on stoichiometry and temperature. In this section, we investigate the vacancy-assisted translation of an APB by using the kMC + Dimer method.

We begin by examining the possible binding of a vacancy to the APB. We placed the vacancy at various sites near three ideal APBs and calculated the binding energy (relative to bulk). The V_{Ni} is only weakly bound (less than 0.1 eV), but the binding of V_{Al} is reasonably strong for (1 1 0) and (1 1 1) orientations (0.35 and 0.30 eV). This leads to the possibility that a vacancy may be both bound to the APB and assist in the reshuffling of atoms at the boundary.

Picture a (1 0 0) APB (as in Fig. 13). If the vacancy is bound to a region near the APB, it might be that the transformation of one region to another would occur easily (as in Fig. 14).

However, we find from the simulations (as described below) that the binding sites are limited, such that to affect a translation of the APB, the vacancy must leave the trap. Therefore, the binding to the APB does not, as one might first think, cause the "zipper" effect described above. Instead, we will find that the mode of action is such that when a vacancy happens to wander by an APB it can accomplish the translation of a portion before it wanders away again. In this way, the AMD simulations are more revealing than simple static calculations of binding energy.

Of course, the conversion of one phase into another is reversible, and in that sense the motion of the APB has itself the character of a random walk. However, in the case where there is some driving force, the random motion of the APB will drift in the direction determined by the driving force, with a velocity which is proportional to the driving force. In the experiments of described in the Introduction, an applied mechanical stress on the dislocation pairs provides a thermodynamic driving force which biases the motion of the APB. In our simulations, we provide a bias in a more direct fashion. To bias the APB motion in one direction, we lowered the saddlepoint energy for vacancy hops which move the APB in a chosen direction, and raise the saddlepoint energy for movements that go in the opposite direction. The bias we used was 0.1 eV.

For these first calculations we set up a periodic Ni₃Al slab of 3456 sites with a pair of (1 0 0) APBs. The slab had dimensions of $6 \times 6 \times 12$ lattice spacings. One vacancy was created, giving a fixed vacancy concentration of
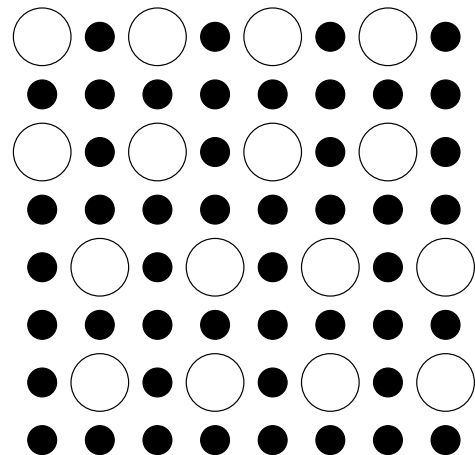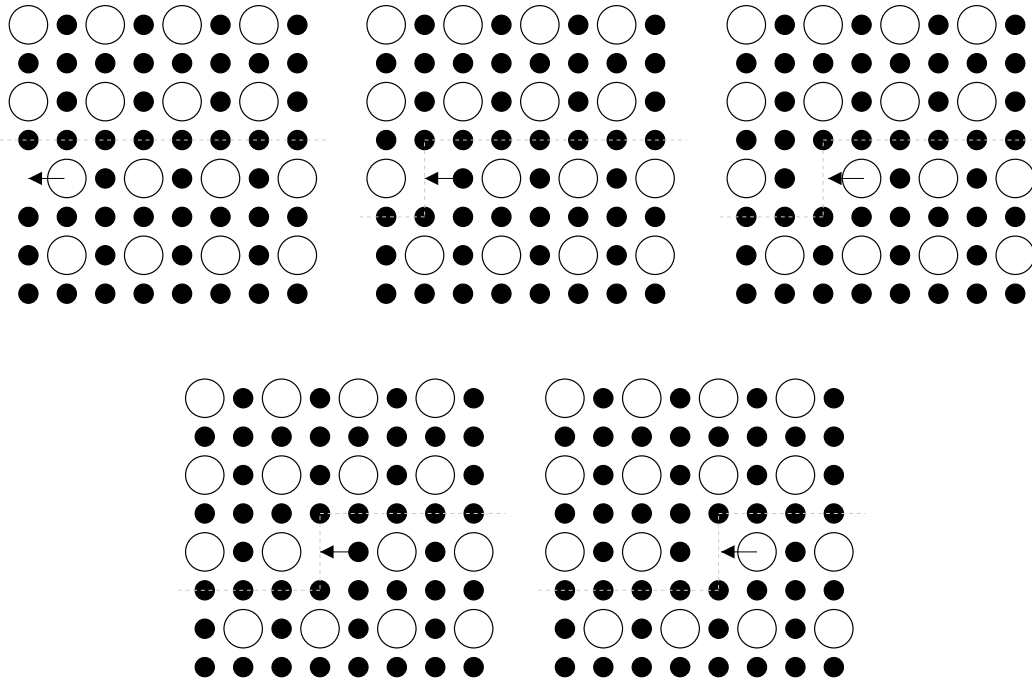

Fig. 13. (1 0 0) APB.

Fig. 14. An example of a sequence of vacancy hops that would translate a (1 0 0) APB.

3×10^{-4}. In this geometry, the APBs are spaced approximately six lattice spacings. (Two APBs are required in order to make the calculation completely periodic.)

The simulation temperature was $T = 900$ K. Each run consisted of 500 kMC steps, and we did a total of 60 runs.

One detail is important to note in this first attempt at a direct simulation of the APB motion. We have set up a slab with ideal composition and no anti-site defects (remembering the APB, of course). In general, one expects that the transition from one phase to another will not be abrupt. Rather, anti-site defects introduced by entropy at high temperature or by pushing the stoichiometry away from ideal will bind to the APB, causing it to be less than abrupt. We have calculated the concentration of anti-site defects that would be present in equilibrium at $T = 900$ K in a sample with ideal stoichiometry. This is done in the same way that bulk defect concentrations were calculated in the previous section (Ref. [8]). We find that at $T = 900$ K and with ideal stoichiometry, the concentration of anti-site defects is negligible (less than 10^{-3}). Thus, for the present temperature and stoichiometry, we feel justified in using an abrupt APB. However, it must be emphasized that if one were to perform the same simulations at higher temperatures or away from ideal stoichiometry, one must consider the higher concentration of anti-site defects at the boundary and the attendant smearing.

We did experiment with seeding the motion of the APB by introducing a step in the APB so that the APB was not completely planar, but that seems to have had little effect on the results.

We find that the simulations do yield motion of the APB, as can be seen in Fig. 15. Our accumulated data show
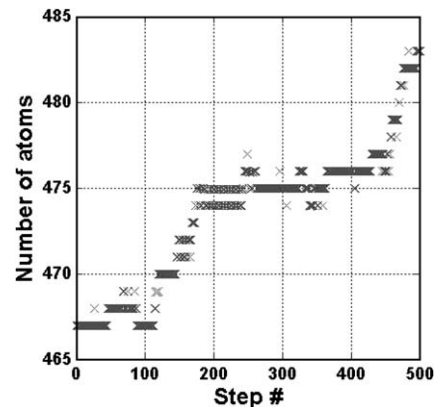

Fig. 15. Plot showing the progression of an APB during biased kMC. The number of atoms in alignment with one side of the APB is plotted vs. iteration.

the velocity of the APB under the bias of 0.1 eV to be $V = 3.7 \pm 2.9 \times 10^3$ Å/s. If the generalized mobility is defined as the velocity divided by the bias, then that gives a value of $\mu = 37 \pm 29 \times 10^3$ Å/(eV s) for an estimate of the mobility.

This is obviously a very low velocity. There are reasons for believing that the APB velocity is strongly temperature and composition dependent. For example, the abrupt APB that exists at the conditions of our calculations (relatively low temperature and ideal composition) might inhibit APB motion because of the difficulties presented for nucleating defects. At higher temperatures or away from ideal stoichiometry, the defects already present at the APB might enable it to be much more mobile. Clearly this is an area for future investigation.

We also have discovered that the direct simulation has an intrinsic weakness: the vacancy spends an appreciable time away from the APB, so that most jumps are not directly related to the APB motion in any way. This is partly why our statistical errors are yet so large. Parallel implementation of the algorithm should help this significantly.

5. Conclusions

We conclude that Accelerated Molecular Dynamics is capable of direct simulation of some diffusion-limited processes. AMD simulations of vacancy diffusion has revealed details of bulk diffusion processes and their dependence on composition and temperature. The more complex process of APB translation has also been investigated at 900 K and ideal stoichiometry, but this case is at the limit of the serial implementation reported in this paper.

We find that the kMC + Dimer method works well at temperatures above 1000 K and for a variety of compositions. The calculated bulk diffusivities compare well with the results of experiment. We also see that kMC + Dimer is alone not sufficient to treat diffusion processes at low temperatures, where the vacancy can become localized by low-energy processes that do not contribute significantly to low-range diffusion.

References

[1] E.P. George, M. Yamaguchi, K.S. Kumar, C.T. Liu, Annu. Rev. Mater. Sci. 24 (1994) 409–451.
[2] T.S. Rong, I.P. Jones, R.E. Smallman, Scripta Metall. Mater. 30 (1994) 19.
[3] R. Srinivasan, M.F. Savage, M.S. Daw, R.D. Noebe, M.J. Mills, Scripta Mater. 39 (1998) 457.
[4] R. Srinivasan, G. Eggeler, M.J. Mills, Acta Mater. 48 (2000) 4867–4878.
[5] See, for example, DIMAT-2000, vols. 194–199.
[6] A.F. Voter, F. Montalenti, T.C. Germann, Annu. Rev. Mater. Res. 32 (2002) 321.
[7] M.S. Daw, S.M. Foiles, M.I. Baskes, Mater. Sci. Rep. 9 (1993) 251.
[8] S.M. Foiles, M.S. Daw, J. Mater. Res. 2 (1987) 5.
[9] A. Voter, S. Chen, Mater. Res. Soc. Symp. Proc. 82 (1987) 175.
[10] K.A. Fichthorn, W.H. Weinberg, J. Chem. Phys. 95 (1991) 1090.
[11] G. Henkelman, H. Jónsson, J. Chem. Phys. 115 (2001) 9657.
[12] Y. Shi, G. Frohberg, H. Wever, Phys. Status Solidi (a) 152 (1995) 361.
[13] K. Badura, U. Brossmann, R. Wurschum, H.E. Shaefer, Mater. Sci. Forum 175–178 (1995) 295.